공학석사학위논문

식물의 움직임을 모사한 수분 반응성 액추에이터의 개발

Development of a hygroscopic soft actuator inspired by botanical movements

2016년 8월

서울대학교 대학원

기계항공공학부

신 범 준

Abstract

Development of a hygroscopic soft actuator inspired by botanical movements

Beomjune Shin

School of Mechanical and Aerospace Engineering

The Graduate School

Seoul National University

It is a general notion that animals are motile but plants are not. Thus, most of efforts to develop biologically inspired robots are focused on mimicking motions of animals. However, some plants generate motions without muscles like animals to generate motions. Plants rely on either supply or deprival of water from plant tissues to make motions. Some species of plants such as wild wheat, *Erodium*, *Pelargonium*, and pinecones can be actuated when the environmental humidity changes. Their tissues are in general composed of highly oriented two layers, one of which is hygroscopically active while the other is inactive. Inspired by this structure, we fabricated an actuator which generates motions in response to humidity change. We newly developed an electrospinning process which can result in a fibrous layer with fast response rate to humidity cahgne. Using this actuator we demonstrated a simple robot

actuated by water vapor, which we named “Hygrobot”.

Keywords: Biomimic, Plants, Hygroscopic swelling, Diffusion, Actuator
Student number: 2014-21856

Contents

List of figures

1. Introduction

It is a general notion that animals are motile but plants are not. Thus, most of efforts to develop biologically inspired robots are focused on mimicking motions of animals[1-3] whether large or not. However, whole plants move as well in order to maximize the robustness of a species although most of their motions are not fast enough to catch with our naked eyes. Movements of plants are fascinating particularly because they do not use muscles like animals to generate motions. Rather, they rely on either supply or deprival of water from plant tissues to make motions,[4, 5] the examples including mimosa leaves,[6] venus flytrap[7] and pine cones[8]. This mechanism is enormously simpler than that of animals using muscles which are composed of complex motor proteins and powered by hydrolysis of ATP.

Some plant species such as Wild wheat[9], *Aristida*, *Pelargonium*[10], *Erodium*[11] and *Stipa* have special seeds which burrow itself into soil using the change of environmental humidity as an energy source. As shown in Fig 1, those self-burial seeds consist of a head containing all the genetic information and a long appendage, called an awn, responsible for locomotion - just like animal sperms. The awns are composed of two tissue layers, one of which swells with humidity (active) but the other is insensitive to humidity change (inactive). If environmental humidity increases, the bilayer bends because of different lengthwise swelling. Periodic change of humidity causes the bilayer to bend and un-bend repeatedly, meaning that environmental humidity energy can be converted to mechanical work.

Recently, a numbers actuators which mimicked moving plants were

reported.[12-15] Some actuator among those bio-inspired robots, some actuator have bilayer configuration, however, unlike the bilayer structures of plant, there are no aligned microstructure. Aligned microstructures in active layer in plants induce anisotropic expansion of bilayer which help plant move pre-programed direction.[16-18] Thus, mimicking bilayers of plants, we here invented a novel bilayer type actuator which has aligned microstructure to maximize its unidirectional expansion. Although the actuator makes bending and un-bending motion in response to humidity change, just repeating those motions makes no net locomotion. In order to fabricate a robot which makes one directional linear locomotion by using this actuator, we have to rectify the repeated motion into a directional one. Joining legs at the ends of the actuator, we fabricated a robot which named “Hygrobot”. Hygrobot makes linear locomotion in response to humidity change without electrical power supply. Furthermore, we analyzed the kinetics of Hygrobot in response to humidity change. We found the optimal design parameter of a Hygrobot which maximizes its speed. This robot shows remarkably fast speed in body length per second compared to other walking robots.

2. Fabrication of Hygroactuator

2.1 Bioinspiration

Plants actuate their organs in various mechanisms. Their motions are largely divided into two types. The first type uses the osmotic influx and efflux of water to make the organs to bend or a specific direction via vacuole of living cells. In this type of plants, they use their own energy to make different osmotic pressure between each cells. And the second type makes motions by using pre-oriented dead tissues (the direction of orientation determined the motions). This type does not use their own energy but use environmental humidity energy. The examples of the first type include Venus flytrap, Mimosa leaf, and phototropism of plants. The second type is evident by the seeds of Wild wheats, Erodium, Ice plants and pine cone. Those examples use the hygroscopic swelling on the awn to achieve specific object, successfully propagate their offspring. Those species exhibit self-burial motion in response to humidity with the awns which attached on their seed. The Ice plant opens its cover and release seeds when the environment is humid enough to the seeds. And the self-burial seed bury itself into the soil to increase the chance to germination.

What makes the passive type plants to generate motions in response to humidity? When we see the cross sectional view of the awns (Fig. 1.1, Fig. 1.2), we can see the clearly divided two layers one of them is hygroscopically active and the other is inactive. The active layer expanses as absorbing water vapour from surroundings while the inactive layer shows no response to water

vapour. Due to well attachment of interface between each layer, swelling of active layer induces the bending deformation of whole bilayer. Particularly each layer which consists the bilayer have a micro structure of well aligned fibers which determines the direction of bending deformation. And the direction of fibers determines the directionality of bending deformation. The awn deforms repeatedly in a programmed direction along the directionality of fibers. The plants rely on the awn to release the seeds due to its robustness and simplicity. To mimic those motility of plants We adopt bilayer configuration, one of whose layers is hygroscopically active while the other is inactive.

The bio-inspired actuators which are actuated by water either in the form of liquid and vapor have been steadily developing. However there exists a feature of the plants which is able to improve the performance of the actuator, the aligned micro structure. We fabricated an actuator which mimic the aligned fibrous structure of plants to maximize the deformation performance.

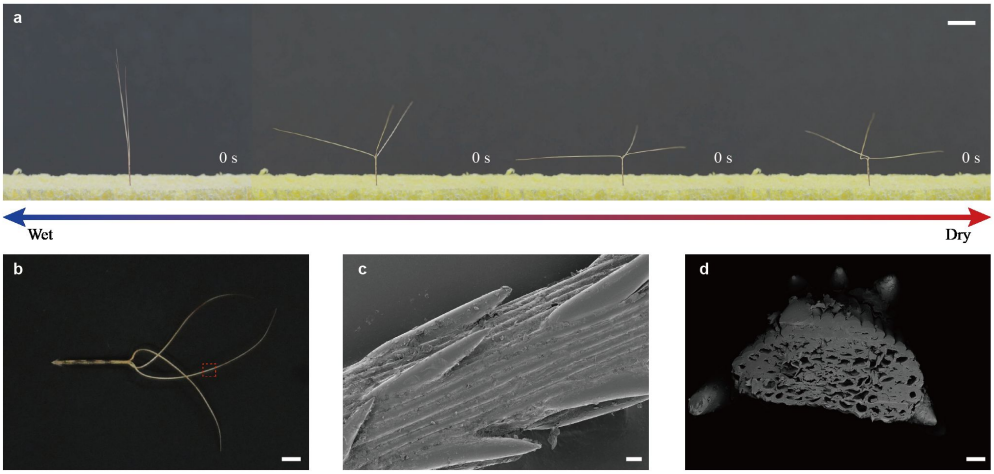

Fig 1.1 (a) Seed of *Aristida* which has three awns generating motility in response to humidity change. (b) The seed consists of head and awns. (c) The awn is composed of micro structure which is made up of hierarchically aligned dead cells. Scale bars represent 5 mm, 3 mm, 200 μm and 200 μm respectively.

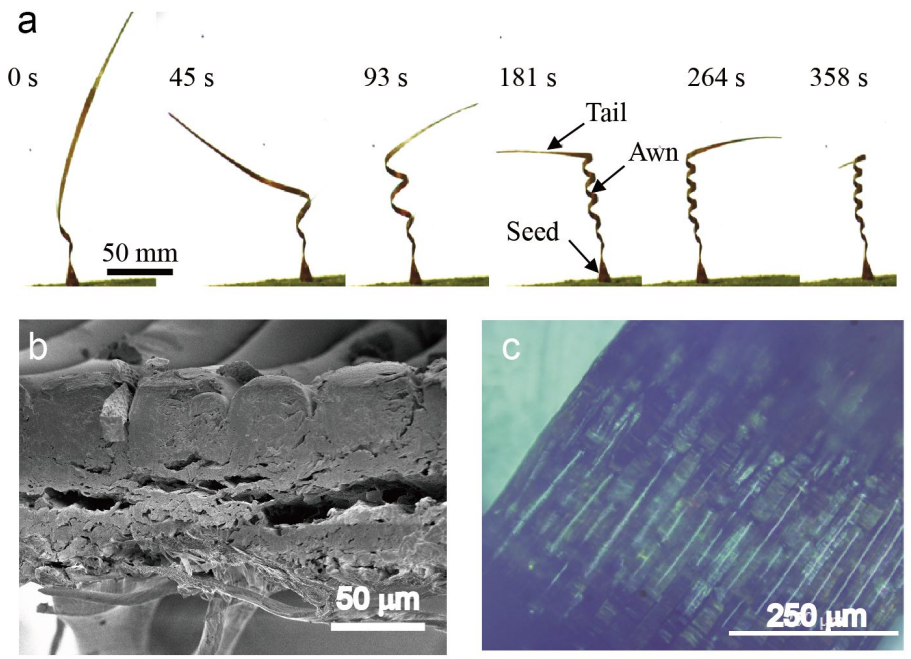

Fig 1.2 (a) Motions of *Pelargonium* seed. When the awn is under humid environment, it is straightened (b) SEM image of the awn. The awn consist of clearly divided two layers. (c) Aligned structure in the awn through optical microscope. [10]

2.2 Fabrication methods

In order to achieve the aligned micro structure which has the similarity to the plants, we adopt electrospinning process to fabricate the hygroscopically active layer. (Fig. 2.1 (a)) During electrospinning process the nano stream of polymer solution erupts randomly. However using a drum collector, which rotates in the same speed with the erupting nanofibers, we can obtain well aligned nano fibrous mesh on the surface of the drum collector. We used hygroscopic material, Polyethylene oxide (PEO) as the polymer solution. After electrospinning, we attached unhygroscopic layer, Polyimide (PI) film, on the nanofibrous mesh, then detached it from the drum collector (Fig 2.1 (b)). The detached bilayer, called “Hygroactuator”, shows bending deformation in response to humidity stimulus. (Fig 2.2 (a)) Through those straightforward steps, we can easily make the Hygroactuator.

As shown in Fig 2.2 (b), the fabricated Hygroactuator has clearly divided two layers. Also, the microstructure of the active layer has well aligned nanofibrous structure. (Fig 2.2 (c)) In response to humidity increase, the nanofibers which consists the active layer expanses in longitudinal direction. While the inactive layer shows no response to humidity change. Because of the difference in reactivity of each layer, the Hygroactuator bends in the direction of PI layer as humidity increases. The Hygroactuator fabricated via aligned electrospinning showed superior deformation angle and response speed as compared to those fabricated via spin-coated hygroscopic materials (Fig 2.2 (d)).

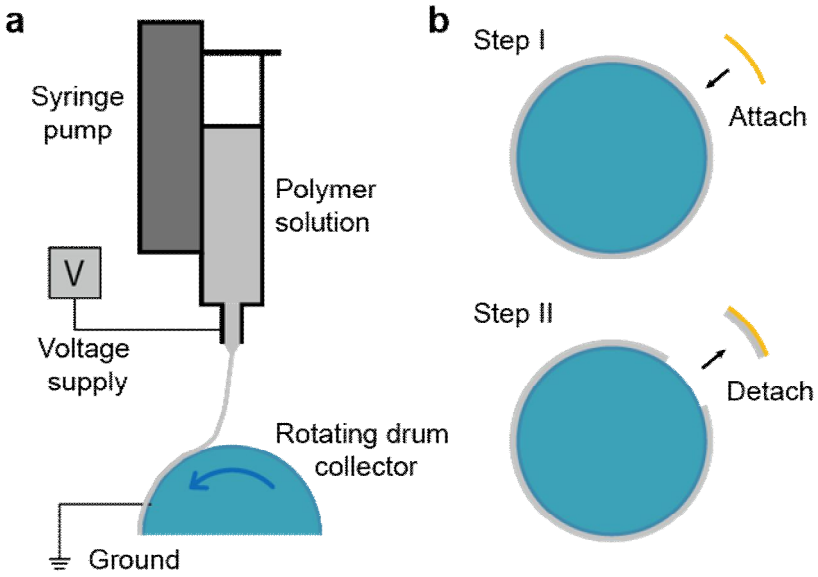

Fig 2.1 (a) The schematics of aligned electrospinning using rotating drum collector. (b) The schematics of fabricating bilayer using electrospun nano fibrous mesh. After electrospinning of PEO, the hygroscopic material, the PI tape, the hygroscopically inactive material, was attached to the fibrous mat (step I). Then the composite layer, which consists of hygrosopically active and inactive layer, is detached from the drum collector.(step II)

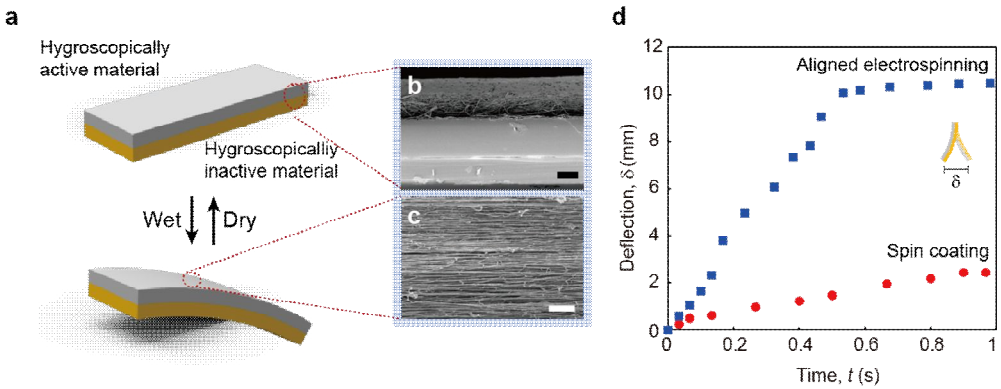

Fig 2.2 (a) The schematics of bilayer actuator. The bilayer response to humidity change. (b) The SEM image of cross-sectional view of the actuator. (c) The aligned structure which was made by aligned electrospinning. Scale bars represents 10 μm and 20 μm respectively.

During electrospinning process, to achieve the hygroscopically active layer, large amount of nanofibers were stacked on the substrate. The surface area to volume ratio of stacked nanofiber mesh is extremely larger than that of spin-coated layer which has more dense micro structure than the super porous electrospun layer. (Fig 2. f) As a result the electrospun active layer shows faster response speed than the spin-coated layer. Furthermore, due to one directionally arranged nanofiber of hygroscopic material, every single fibers expanses in the equivalent longitudinal direction without disturbing each other to be expanded. Consequently, the net bending deformation of the actuator improved compared to the actuators which made by conventional method.

3. Analysis of Hygroactuator

3.1 Diffusion model

To elucidate the bending deformation of the actuator in response to humidity change according to time, we focused on the driving force of the actuator, diffusion of humidity. As the humidity increases, the characteristics of the layer which was made with hygroscopic material changes. The amount of hygroscopic swelling increases in proportional to humidity and hygroscopic swelling ratio. The Young's modulus decreases as humidity increases.

When the humidity around the actuator becomes higher, the moisture molecules are not able to pass through the inactive layer, while easily penetrate into the electrospun active layer. According to the difference of moisture permeability, the moisture starts diffusion into the vertical direction of the actuator from the outer side of active layer. Thus, we assumed that the bilayer follows one-dimensional diffusion with insulated end. As following our assumption, the diffusion equation,

$$\frac{\partial \phi}{\partial t} = D\frac{\partial^2 \phi}{\partial z^2} \tag{1}$$

governs the phenomena. The notation t, ϕ, D and z represent time, humidity, diffusivity, distance from z-axis basement. The initial condition is $\phi(z,0) = \phi_0$, while the boundary conditions are $\phi(0,t) = \phi_\infty$ at the outer surface of active layer and $\partial\phi/\partial z = 0$ as the interface between active and inactive layer $(z = L)$ where ϕ_0 and ϕ_∞ represents initial humidity and

changed humidity respectively. The solution is obtained by the separation of variables as follows.

$$\phi(z,t) = \sum_{n=1}^{\infty} \left(\frac{-2(\phi_0 - \phi_\infty)}{(n+\frac{1}{2})\pi} sin \frac{(n+\frac{1}{2})\pi}{L} z e^{-\lambda_n^2 t} \right) + \phi_\infty \qquad (2)$$

3.2 Discretized multi-layer model

During moisture diffusion, vertical humidity distribution along the normal direction of the layer formed in the active layer at each instants. We assumed the active layer as a discretized multi-layer that every layer has discontinuous humidity distribution. As shown in Fig. 3.1 a, the layer 1 and the other layers represent the hygroscopically inactive and active layer respectively. We can define the curvature with a model which is based on the classical beam theory[19, 20]. The pure bending strain, ϵ_b that cantilever structure without any external load takes is obtained as $\epsilon_b = \epsilon_0 - z\kappa$. Where ϵ_0 is the reference strain at the reference plane, z is the distance from reference plane and κ is the bending curvature. When the actuator faces humid ambient, the active layer of the actuator swells. Then, the hygroscopic swelling induces hygroscopic strain α. Thus, the total strain, which is applied to the bilayer actuator, is derived from the different between geometric and hygroscopic strain, $\epsilon = \epsilon_b - \alpha = \epsilon_0 - z\kappa - \alpha$. From the strain we can obtain the bending force F and bending moment M by integrating stress, $\sigma = E\epsilon = E(\epsilon_0 - z\kappa - \alpha)$, along the cross section of layers.

$$F = \int \sigma dz = \int E(\epsilon_0 - z\kappa - \alpha)dz \tag{3}$$

$$M = \int \sigma z dz = \int E(\epsilon_0 - z\kappa - \alpha)z dz \tag{4}$$

Without any external loads the force and moment is zero at equilibrium state.

Then, $A\epsilon_0 - B\kappa = F_\alpha$ and $B\epsilon_0 - D\kappa = M_\alpha$, where A represents extensional stiffness, B represents bending-extension stiffness and D represents bending stiffness. We compute the equations through numerical integration along each layers. Thus each stiffness, force and moment become as follows.

$$A = \int E dz = E_1 h_1 \sum_{i=1}^{N} m_i n_i \tag{5}$$

$$B = \int E z dz = \frac{E_1 h_1^2}{2} \sum_{i=1}^{N} (m_i^2 + 2 m_i p_i) n_i \tag{6}$$

$$D = \int E z^2 dz = \frac{E_1 h_1^3}{3} \sum_{i=1}^{N} (m_i^3 + 3 m_i^2 p_i + 3 m_i p_i^2) n_i \tag{7}$$

$$F_\alpha = \int E \alpha dz = E_1 h_1 \sum_{i=1}^{N} m_i n_i \alpha_i \tag{8}$$

$$M_\alpha = \int E \alpha z dz = \frac{E_1 h_1^2}{2} \sum_{i=1}^{N} (m_i^2 + 2 m_i p_i) n_i \alpha_i \tag{9}$$

Where $m_i = h_i / h_1$, $n_i = E_i / E_1$, $p_i = z_i / h_1$, and N is the total number of layers. So, we can obtain curvature as follows.

$$\kappa = \frac{AM - BF}{B^2 - AD} \tag{10}$$

In the equation Young's modulus E and hygroscopic strain α varies according to relative humidity. Thus coupling with above mentioned humidity distribution, we can predict the curvature of the bilayer actuator induced by humidity change at each instants. (Fig 3.1 (b)) In the case of various active

layer thickness, our model well explained the bending deformation of the bilayer as shown in Fig 3.1 (b)

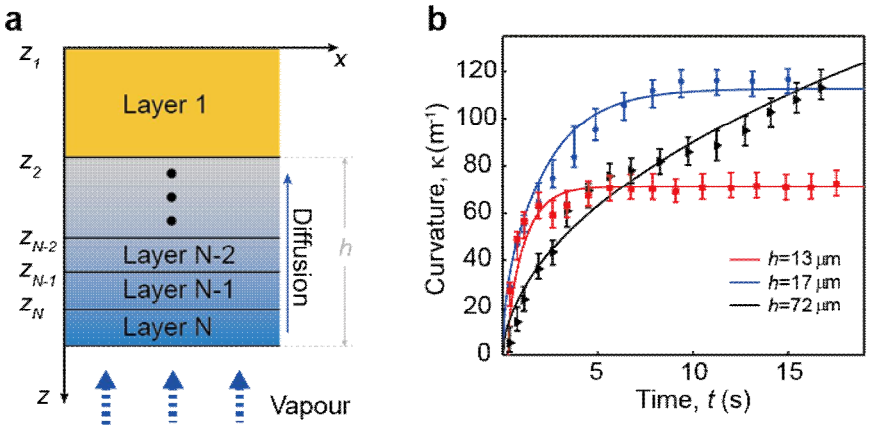

Fig 3.1 (a) The dicretized multilayer model. (b) The graph which includes validation with experiments.

4. Hygrobot

4.1 Fabrication of Hygrobot

We fabricated Hygrobot via attaching legs at the ends of the bilayer actuator to guide the direction. Hygrobot we made is capable of locomotion only by environmental humidity change, needing no electrical power supply. The legs are made up of PET film. In order to make two contact mode it was bended twice as shown in Fig. 4.1 (b). Mode I and mode II represents the state that thin end of the leg makes contact with substrate and bent part makes contact with substrate respectively. Owing to the aspect of contact mode, the ratchet shows higher friction force in mode I compared to mode II. While the actuator repeats bending and unbending, the fore leg and hind leg changes their contact mode to the substrate.

To quantify the foregoing speed of Hygrobot, we actuated it with a constant periodic change of humidity as shown in Fig 4.1 (c) The supplement of humidity was controlled following step function by programmed automatic humidity changer. To make precise input humidity change, we used an automated humidity changer which is programmed to generate periodic humidity change following step function. First the Hygrobot starts with dry condition, the actuator has convex shape down. In this state, the fore leg and the hind leg takes mode I and mode II respectively. (Fig 4.1 (a)) As humidity increases, the active layer becomes absorbed by moisture, the actuator bends. Thereby the actuator becomes convex to the top and both legs subjected to a force which is drawn on the inside of the legs. But only hind leg is dragged

to forward. Because the friction force of fore leg is bigger than that of hind leg, the fore leg takes its original position while the hind leg does not. During this change, the fore leg alters its contact mode I to II and the hind leg alters vice versa. Passes into dry condition again, the active layer passes through the desiccation state and changes in the shape of a convex downward. Each legs receives a force which pushes the legs outward. During this change, the hind and fore leg in under the mode I and II respectively. Thus, the hind leg is fixed while the fore leg is advancing forward. By repeating this sequence, Hygrobot makes foregoing locomotion.

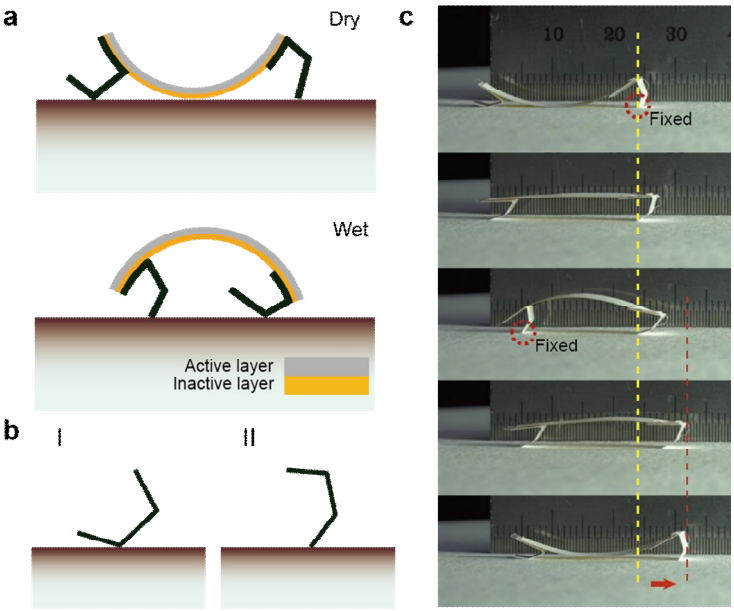

Fig 4.1 (a) The schematics of Hygrobot on the dry and wet atmosphere respectively. (b) Two contact mode of the ratchet which were joined to bilayer actuator. (c) The timelaps of the Hygrobot.

4.2 Velocity of Hygrobot

The propelling speed of Hygrobot can be defined as how many distance propelled during one period. The distance traveled during one period can be expressed by the change in projection length due to the bending deformation of the actuator. The projection length can be easily derived geometrically from the curvature of the actuator. As shown in Fig 4.2, the change in projection length Δl is the differences between l, body length of the Hygrobot and l_p, the projection length of bended Hygrobot. The projection length, $l_p = 2/\kappa \sin(l\kappa/2)$. Thus, the propelling speed, v becomes $v = \Delta l/\tau = (1-2/\kappa \sin(l\kappa/2))/\tau$. We also identified our model with various thickness of active layer and the actuating period.

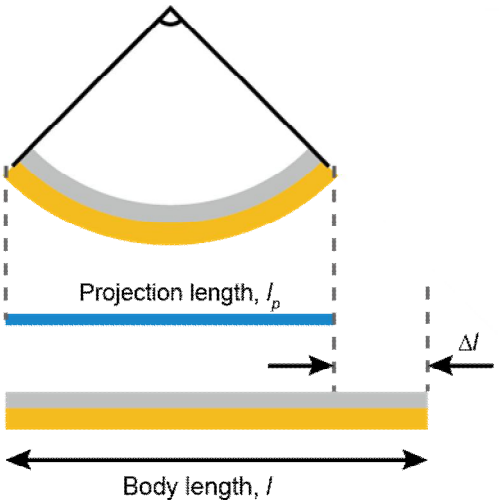

Fig 4.2 The schematics of projection length derived from the bending curvature of the bilayer actuator.

4.3 Optimal design for the fastest Hygrobot

By coupling the humidity distribution at each instants and bending curvature induced by humidity change, with given robot size, length and width are given at 25 mm and 3 mm, we numerically obtained dependency of the velocity of hygrobot on τ and h as shown in Fig 4.3 (a). In the fixed active layer thickness case (Fig. 4.3 (b)), as the period of humidity change is shorter, the velocity of hygrobot increases. Our model well matches with the experimental data except the short period region. When the Hygrobot is actuated with a notoriously short period, the Hygrobot is not able to generate a sufficient deformation for the ratchet to be operated. When the actuation period is fixed (Fig. 4.3 (c)), we found that our Hygrobot speed is maximized when a thickness of active layer is $\sim$ 30 μm. The thickness which is predicted by our model is different from that of maximum bending curvature predicted by a Timoshenko's bimetal model. Timoshenko's bimetal model is focused on metallic bilayer which responds to heat change. The heat diffusivity of metallic materials are higher than moisture diffusivity of hygroscopic polymer materials. Thus, the diffusion of heat in the bimetal occurs in an instant while time required of Hygroactuator is long enough to be considered. Hence, the thickness of active layer which maximize the bending curvature according to time is identified as shown in Fig 4.3 (c).

Using our analytical model, if the period of humidity change is 1s, we have obtained that the fastest Hygrobot moves in 2.9 mm/s.

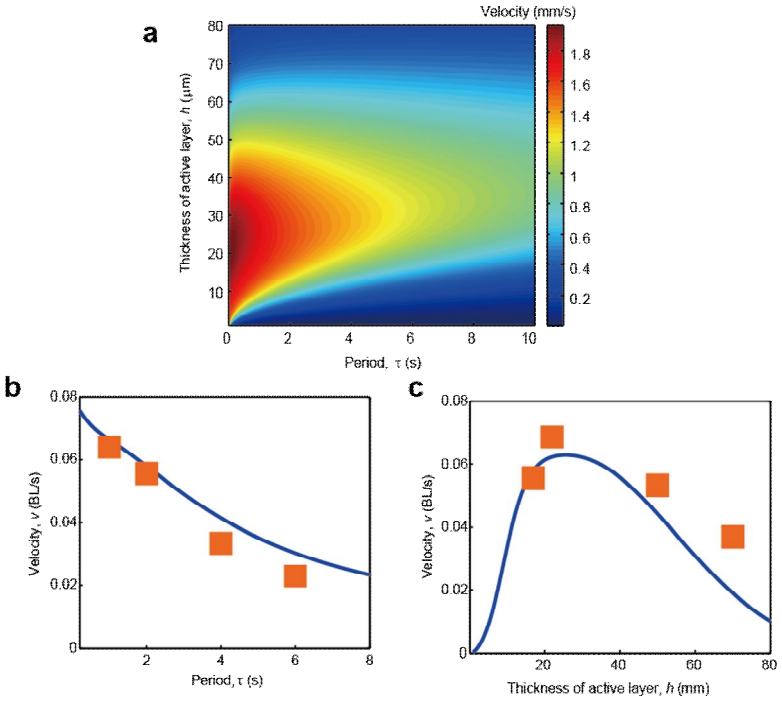

Fig 4.3 (a) The velocity map according to thickness of active layer and the period of humidity change. (b) The velocity profile of Hygrobot according to period of humidity change at fixed thickness of active layer. (c) The velocity profile of Hygrobot according to thickness of active layer at fixed period of humidity change.

4.4 Comparisons

When we compared the absolute speed of Hygrobot with other soft robots, Hygrobot moves not that fast. (Fig 4.4 (a)) However, using the unit, body length per second, which is commonly used in comparing the speed between various species of animals, Hygrobot shows 0.085 BL/s, it is faster than other soft robots. Plus, animals and existing robots which generate walking motions have a certain tendency between velocity and mass each (Fig 4.4 (b)). The artificial robots are located under the animals of nature. The heavier ones almost catch up performance of the nature but the lighter ones take far below the nature. Our Hygrobot takes elevated site on the graph.

In conclusion, by mimicking aligned micro structure of a particular spices of plants, we fabricated an actuator which makes fast and large deformation in response to humidity change. Furthermore, Hygrobot, which actuated by the change of humidity, demonstrate the possibility that the actuator can be used on robots. Hygrobot shows the fastest speed compared to other walking robots available today when measured body length per second even without electrical energy supply. Also, it shows remarkable progress in the area of velocity per mass. The speed per mass of large robots beats that of animals whereas that of small robots far below the animals. There is a certain advancement of velocity per mass in Hygrobot. Our technology can lead to micro-robots that can work only with environmental humidity change in the field where lacks of the energy source. The humidity change occurs everywhere around us, even when we breathe humid air exhaled. Thus, using humidity which disappears even now around us, we make tremendous motions with the Hygrobot.

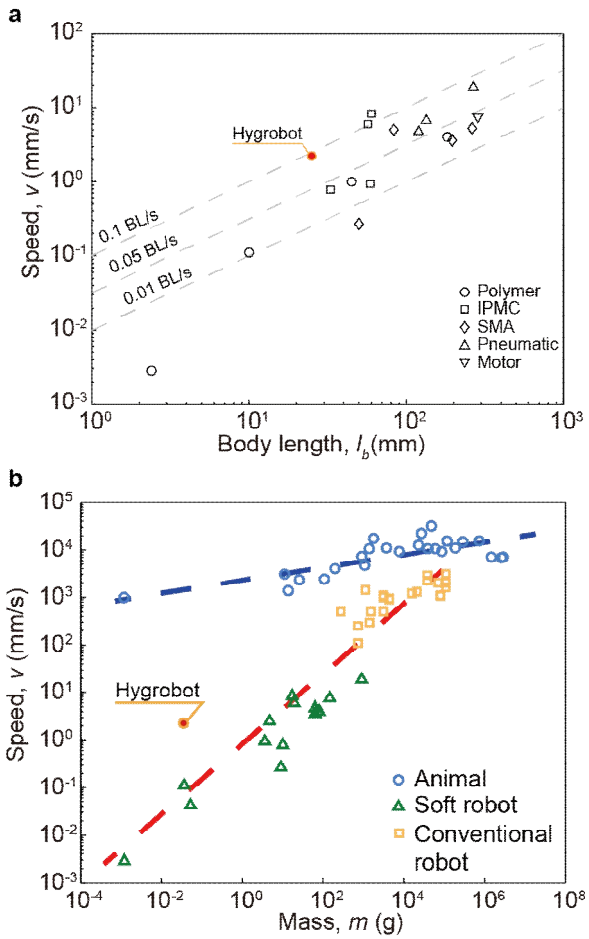

Fig 4.4 (a) The comparison with other soft robots (b) The comparison with other soft robots, conventional robots and bipedal animals.

5. Conclusions

In conclusion, by mimicking aligned micro structure of a particular spices of plants, we fabricated an actuator which makes fast and large deformation in response to humidity change. Furthermore, Hygrobot, which actuated by the change of humidity, demonstrate the possibility that the actuator can be used on robots. Hygrobot shows the fastest speed compared to other walking robots available today when measured body length per second even without electrical energy supply. Also, it shows remarkable progress in the area of velocity per mass. The speed per mass of large robots beats that of animals whereas that of small robots far below the animals. There is a certain advancement of velocity per mass in Hygrobot. Our technology can lead to micro-robots that can work only with environmental humidity change in the field where lacks of the energy source. The humidity change occurs everywhere around us, even when we breathe humid air exhaled. Thus, using humidity which disappears even now around us, we make tremendous motions with the Hygrobot.

References

1. Seok, S. et al. Meshworm: A Peristaltic Soft Robot With Antagonistic Nickel Titanium Coil Actuators. IEEE/ASME Transactions on Mechatronics 18, 1485-1497 (2013).

2. Hatton, R. L. & Choset, H. Generating gaits for snake robots: annealed chain fitting and keyframe wave extraction. Autonomous Robots 28, 271-281 (2010).

3. Kovac, M., Fuchs, M., Guignard, A., Zufferey, J.-C. & Floreano, D. in Robotics and Automation, 2008. ICRA 2008. IEEE International Conference on. 373-378 (2008).

4. Burgert, I. & Fratzl, P. Actuation systems in plants as prototypes for bioinspired devices. Philosophical transactions. Series A, Mathematical, physical, and engineering sciences 367, 1541-1557 (2009).

5. Forterre, Y. Slow, fast and furious: understanding the physics of plant movements. Journal of experimental botany (2013).

6. Satter, R. L. & Galston, A. W. Mechanisms of control of leaf movements. Annual Review of Plant Physiology 32, 83-110 (1981).

7. Forterre, Y., Skotheim, J. M., Dumais, J. & Mahadevan, L. How the Venus

flytrap snaps. Nature 433, 421-425 (2005).

8. Dawson, C., Vincent, J. F. & Rocca, A.-M. How pine cones open. Nature 390, 668-668 (1997).

9. Elbaum, R., Zaltzman, L., Burgert, I. & Fratzl, P. The role of wheat awns in the seed dispersal unit. Science 316, 884-886 (2007).

10. Jung, W., Kim, W. & Kim, H.-Y. Self-burial mechanics of hygroscopically responsive awns. *Integrative and comparative biology*, 026 (2014).

11. Stamp, N. E. Self-burial behaviour of Erodium cicutarium seeds. The Journal of Ecology, 611-620 (1984).

12. Chen, X. et al. Scaling up nanoscale water-driven energy conversion into evaporation-driven engines and generators. Nature communications 6, 7346 (2015).

13. Chen, X., Mahadevan, L., Driks, A. & Sahin, O. Bacillus spores as building blocks for stimuli-responsive materials and nanogenerators. Nature nanotechnology 9, 137-141 (2014).

14. Chen, P. et al. Hierarchically arranged helical fibre actuators driven by solvents and vapours. Nature nanotechnology (2015).

15. Reyssat, E. & Mahadevan, L. Hygromorphs: from pine cones to

biomimetic bilayers. Journal of the Royal Society Interface (2009).

16. Fratzl, P., Elbaum, R. & Burgert, I. Cellulose fibrils direct plant organ movements. Faraday Discussions 139, 275 (2008).

17. Abraham, Y. et al. Tilted cellulose arrangement as a novel mechanism for hygroscopic coiling in the stork's bill awn. Journal of the Royal Society, Interface / the Royal Society 9, 640-647 (2012).

18. Erb, R. M., Sander, J. S., Grisch, R. & Studart, A. R. Self-shaping composites with programmable bioinspired microstructures. Nature communications 4, 1712 (2013).

19. Timoshenko, S. Analysis of bi-metal thermostats. JOSA 11, 233-255 (1925).

20. Du, P., Lin, X. & Zhang, X. A multilayer bending model for conducting polymer actuators. Sensors and Actuators A: Physical 163, 240-246 (2010).

국 문 초 록

흔히 우리는 움직임을 보이는 생명체를 떠올릴 때 동물을 생각한다. 이러한 관념 속에서 대부분의 생체모사 로봇의 개발은 그 크기가 크건 작건 동물의 움직임을 모사하는데 집중되어왔다. 그러나 식물은 비록 그 움직임이 느려서 우리가 눈치 채기 힘들지만 움직임을 만든다. 특히 식물의 움직임을 만드는 방식은 동물이 움직임을 만들기 위해서 복잡한 화학작용을 통해 운동성을 만들어내는 근육을 사용하지 않는 다는 점에서 많은 가능성을 가진다. 대신 그들은 다양한 방법으로 그들의 조직 내의 물의 공급과 제거를 통해서 움직임을 만든다. 이러한 식물의 움직임의 예로는 파리지옥, 미모사, 솔방울 등이 있다. 우리는 자가 매립을 하는 *Erodium*, *Pelargonium*, *Aristida* 등의 식물의 씨앗이 가진 특별한 구조인 정렬되어 있는 섬유다발의 집합으로 만들어진 이중층 구조를 모사하여 주변 수분에 반응하여 움직임을 만드는 액추에이터를 제작하였다. 이 액추에이터는 바이메탈의 변형과 흡사하게, 수분에 대한 변형량이 다른 흡습성층과 비 흡습성층이 접합되어 있고, 주변의 수분 변화에 따라 굽힘 변형을 만들어서 운동성을 만든다. 제작 과정에서 전기방사를 도입하여 식물이 가진 정렬되어 있는 섬유 다발의 모사하였고, 이를 통해 액추에이터는 극대화된 변형을 보였으며, 나노섬유의 높은 부피 대비 표면적 비로 인해 수분 변화에 대해 빠른 반응을 보였다. 우리

는 이 액추에이터를 이용하여 수분의 변화로 직선 운동을 할 수 있는 로봇, “하이그로봇”을 제작하였다. 우리는 액추에이터의 성능을 평가하는 지표로써 굽힘에 의한 곡률을 이용하였고, 수분의 확산에 의해서 시간에 따라 곡률이 어떻게 변하는지 밝혀냈다. 또, 이를 통해 하이그로봇의 속도를 유추할 수 있었고, 최대의 속도를 만들 수 있는 흡습성 층의 두께를 찾아냈다. 최적의 조건으로 만들어진 하이그로봇은 절대 속도는 빠르지 않으나 몸길이를 고려하여 다른 로봇들과 비교하였을 때 대단히 빠른 속도로 움직였다.

주요어: 식물모사, 습윤 팽창, 확산, 액추에이터
학 번: 2014-21856